Inferring the location of reflecting surfaces exploiting loudspeaker directivity

Zaccà, V.G.; Martínez-Nuevo, Pablo ; Møller, Martin Bo ; Martinez, Jorge; Heusdens, R.

Publication date
2020

Document Version
Final published version

Published in
Proceedings of the 28th European Signal Processing Conference, EUSIPCO

Inferring the location of reflecting surfaces exploiting loudspeaker directivity

Vincenzo Zaccà*† Pablo Martínez-Nuevo* Martin Møller* Jorge Martínez† and Richard Heusdens†
*Bang & Olufsen, †Delft University of Technology

***Abstract*—Accurate sound field reproduction in rooms is often limited by the lack of knowledge of the room characteristics. Information about the room shape or nearby reflecting boundaries can, in principle, be used to improve the accuracy of the reproduction. In this paper, we propose a method to infer the location of nearby reflecting boundaries from measurements on a microphone array. As opposed to traditional methods, we explicitly exploit the loudspeaker directivity model—beyond omnidirectional radiation—and the microphone array geometry. This approach does not require noiseless timing information of the echoes as input, nor a tailored loudspeaker-wall-microphone measurement step. Simulations show the proposed model outperforms current methods that disregard directivity in reverberant environments.**

***Index Terms*—Room geometry estimation, sparse recovery, beamforming, room acoustics, image source model, spatial room impulse response, loudspeaker directivity model**

I. Introduction

The sound field produced by a loudspeaker system in an enclosed space is primarily—but not exclusively—determined by the loudspeakers characteristics and their position relative to the room walls [1]. "Smart" loudspeakers including built-in microphone arrays are becoming ubiquitous. Often sound field reproduction using these high-end systems has to comply with strict quality requirements: The listening experience should be good irrespective of where the loudspeaker is placed in the room. Reflections of sound from the surfaces in the room — the locations of which are unknown in practice — result in inaccurate sound reproduction [2]. One could try to infer a total or partial estimate of the room shape using the built-in microphones, and use this information to improve the quality of the sound field generated by the loudspeaker system.

The problem addressed in this paper is the following: given a system composed of a co-located microphone array of known geometry and a co-located loudspeaker set with known directivity; estimate the location of reflecting surfaces close to the system.

Existing methods that estimate the location of reflecting surfaces by emitting a known signal using a loudspeaker are classically carried out as follows: First, the room impulse response (RIR) is estimated as a step in calculating the time of arrival (TOA). GCC-PHAT [3] is an established algorithm to achieve this. Further consider a compact microphone array, beamforming can be used to calculate a steered-response. This results in improved robustness against uniform spatially uncorrelated noise. In this setting, the microphone array geometry can be exploited as prior for the TOA estimation. In a scenario where the echoes need to be sorted, greedy methods are often used [4], [5]. The performance of these methods usually degrades with reverberation—i.e. reflecting boundaries—, especially when received echoes have overlap in time (which happens due to finite measurement bandwidth). Moreover, the echo sorting problem is computationally demanding.

The problem can be relaxed by including information about the loudspeaker-wall behavior and solving the source localization problem jointly. In particular, explicit loudspeaker modeling is often neglected and simplified to omnidirectional or highly directive models [6]. In [7], the loudspeaker-wall interaction is implicitly considered by constructing a dictionary from experimental measurements. That method improves performance in an ideal scenario, but it is not robust when the scenario deviates from the measured dictionary.

In this paper, we propose a measurement model that explicitly includes loudspeaker directivity and the microphone array geometry. We use this model to solve an inverse problem: from microphone measurements it outputs an estimation of the nearby reflecting boundaries. This approach does not require noiseless timing information of reflections, nor a tailored loudspeaker-wall-microphone measurement dictionary. As indicated by the simulations, the proposed algorithm shows improved performance compared to current methods that disregard loudspeaker directivity.

II. Proposed method

We propose a novel microphone signal model that maps the location of image sources to microphone measurements. Then, the problem of estimating the location of reflecting surfaces is solved as an inverse problem. We first describe the signal model in the continuous domain. After discretization it is reformulated in matrix-vector form. Finally, the inverse problem is posed as an ℓ_1-regularized convex optimization problem.

Similar to the image source method [8], our signal model is based on geometric acoustics, i.e. the concept of sound waves is replaced by sound rays that travel in a narrow path and reflect specularly. We assume that all image sources lie on a horizontal plane in order to model vertical planar surfaces in the room. Although presumably extensible to three dimensions, we consider for simplicity that the ceiling and floor reflectors fully absorb. We further assume that the center of the loudspeaker system lies at the origin, thus coinciding with the geometric center of a uniform circular array.

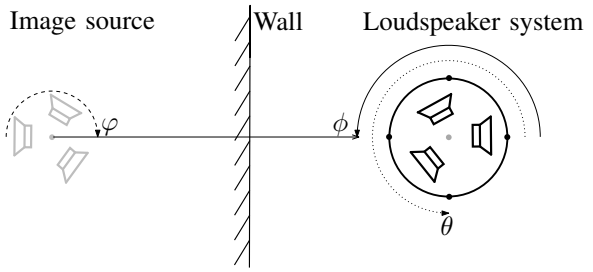

Fig. 1: Model setup. To the right a loudspeaker system and a circular microphone array. The center dot represents the origin of coordinates. To the left an image source that models sound reflection. A reflected sound ray is depicted. The angles ϕ, φ, and θ denote the angle of the image source position, the emission angle, and the angle representing a position on the microphone array, respectively.

A. Continuous Measurement Model

Our model is determined by three main components: Specular reflection modeled by equivalent image sources, a loudspeaker with a non-homogeneous directivity response, and a co-located circular microphone array. Consider the set $\mathcal{S}$ containing the spatial locations of K image sources of first order, i.e. $\mathcal{S} = \{\mathbf{r}_k\}_{k=0}^{K-1}$ for $\mathbf{r}_k \in \mathbb{R}^2$ and $K > 0$. In this work we restrict ourselves to first-order images since we are considering only dominant reflections. In general the contributions of these sources dominate the early part of the room impulse response. For convenience spatial locations are expressed in polar coordinates, i.e. $\mathbf{r} = (R, \phi)$, for $R \in \mathbb{R}_+$ and $\phi \in \mathcal{E} = [0, 2\pi)$ the angular support.

We start the analysis describing a theoretical circular array with a continuous aperture. A practical microphone array is later modeled by sampling the continuous aperture in space. Let the signal received by the continuous array be denoted by $y(t, \theta)$, with $\theta \in \mathcal{E}$. Here we assume a fixed array radius. Dependence on the radius is therefore not stated explicitly. The signal model is given by the following map:

$$\begin{aligned} \mathbb{R}^2 &\rightarrow L^2(\mathbb{R}, \mathcal{E}) \\ \mathcal{S} &\mapsto y(t, \theta), \end{aligned} \tag{1}$$

where L^2 is Lebesgue's space of finite energy signals. In this paper, the goal is to obtain an approximation of the inverse of the map stated in (1), i.e. to recover the image source locations from signal measurements at different angles (i.e. array positions). In later sections we show that the inverse problem can be posed as a convex optimization problem in the discrete domain. The three main components of our model are introduced next.

1) Image Source locations: The loudspeaker system emits a known signal $x(t)$. The sound is reflected specularly at a wall. Estimation of the source location is derived from an estimation of the wall's position. This is depicted in Fig. 1. The received signal y can be written as

$$y(t, \theta) = \left(x * \left(h_{\text{dp}}(\cdot, \theta) + \sum_{\mathbf{r} \in \mathcal{S}} h_s(\cdot, \theta, \mathbf{r}) \right) \right)(t), \tag{2}$$

where $*$ denotes convolution, $h_{\text{dp}}(t, \theta)$ is the channel response of the direct path from the loudspeaker to a microphone located at θ, and $h_s(t, \theta, \mathbf{r})$ models the path from an image source to a point on the circular array. The direction of arrival of sound rays corresponding to first (and in some cases second) order reflections coincides with the angle formed by the wall's normal point and the center of the array, as seen in Fig. 1.

2) Loudspeaker Directivity: Let us define an angle-dependent loudspeaker system response in the far-field (at a distance R_0), and denote it by $\gamma_0(t, \varphi)$, where $\varphi \in \mathcal{E}$. We assume this function is known (e.g. it has been measured a priori), and the system is linear time-invariant. Then we can extrapolate the loudspeaker impulse response at distances $R > 0$,

$$\frac{R_0}{R} \gamma_0 \left(t - \frac{R - R_0}{v_c}, \varphi \right), \tag{3}$$

where v_c denotes the speed of sound in m/s which is assumed constant and known. Note that (3) constitutes a (simplified) model for loudspeaker system directivity.

3) Circular-array response: Without loss of generality we set the center of the circular array at the origin of coordinates. Image sources are assumed to be in the far field. It is therefore reasonable to assume signal attenuation due to the distance is approximately equal at all positions on the array's circumference. The array response is then determined by relative delays between positions on the circumference. These delays can be inferred from the direction of arrival of incoming sound, and the array geometry. For the uniform circular array, it is easy to show, referring to (2) and (3), that [9], [10]

$$h_s(t, \theta, R, \phi) = \frac{R_0}{R} \gamma_0 \left(t - \frac{R - R_0}{v_c} - \frac{R_a}{v_c} \cos(\theta - \phi), \phi \right), \tag{4}$$

where R_a is the radius of the array. For this particular geometry and image source set $\mathcal{S}$, the angle $\varphi = \phi$ in Eq. (4). The function $h_s(t, \theta, R, \phi)$ represents the response (including loudspeaker directivity) at an angle θ in the array due to a image source located at $\mathbf{r}$ (recall that $\mathbf{r} = (R, \phi)$). In an enclosed space (e.g, a room), the channel response including all sources contributions is given by $h(t, \theta) := \sum_{\mathbf{r} \in \mathcal{S}} h_s(t, \theta, R, \phi)$. Let us now express h as a convolution integral, this is

$$h(t, \theta) = \int_{\mathcal{E}} \int_{\mathbb{R}_+} h_s(t, \theta, R', \phi') u_{\mathcal{S}}(R', \phi') \mathrm{d}R' \mathrm{d}\phi', \tag{5}$$

where $u_{\mathcal{S}}(R, \phi) := \sum_{\mathbf{r}' \in \mathcal{S}} (R_0/R) \delta(R - R', \phi - \phi')$. The key observation is that the above can be decomposed as three convolutions:

$$\begin{aligned} h(t, \theta) = \int_{\mathbb{R}} \int_{\mathcal{E}} \delta \left(t - t' - \frac{R_a}{v_c} \cos(\theta - \phi') \right) \\ \int_{\mathbb{R}_+} \gamma_0(t' - \frac{R' - R_0}{v_c}, \phi') u_{\mathcal{S}}(R', \phi') \, \mathrm{d}R' \mathrm{d}\phi' \mathrm{d}t', \end{aligned} \tag{6}$$

which can be interpreted as a linear convolution in time—proportional to distance—to extrapolate the loudspeaker impulse response, and a two-dimensional convolution to compute the relative microphone delays. In the next section, we discretize (6) and reformulate it in matrix-vector form.

B. Discrete Measurement Model

The system defined by $h(t,\theta)$ is described by the model's three main components: the image source locations, the directivity information of the loudspeaker, and the influence of the microphone array geometry. It is further assumed that we can know a reasonably accurate discrete version of $h(t,\theta)$, the array geometry, and the loudspeaker's directivity. We then aim at exploiting this information in order to find the image source locations corresponding to the dominant reflecting boundaries. Note first that in a real scenario it is necessary to have a preprocessing stage. In particular, with the right choice of excitation signals it is possible to perform an accurate deconvolution [11]. Moreover the direct path $h_{\text{dp}}(t,\theta)$, can in principle be estimated from anechoic measurements and be subtracted from the process.

We consider that the input to our system is a discrete version of $h(t,\theta)$ denoted by $h[n,m]$ for time steps $n = 0,\dots,N_h-1$ and microphone indexes $m = 0,\dots,M-1$. In other words, we assume we can obtain $h[n,m]$ from measurements $y(t,\theta)$. We show below how to decompose this system into its three different building blocks.

1) Image Source Locations: We first discretize $\mathbb{R}^2$ uniformly in polar coordinates. Our microphone measurements are sampled in time at f_s Hz for M distinct microphones. We use a stepsize for the radial distance of $\Delta R = v_c/f_s$, and an angular stepsize $\Delta\theta = 2\pi/(MP)$ for some integer $P \geq 1$ representing an upsampling factor in the angle domain. We restrict the image source distances to a range between $R_{\min} = R_a$ and $R_{\max} = Tv_c/f_s + R_a$ for some integer $T \geq 1$. Image source locations are then assigned to the closest point in this discretized set. We create the corresponding Voronoi regions in $\mathbb{R}^2$ by using this discrete set of points as generators. Thus, we have TMP Voronoi regions denoted as $V(\mathbf{g})$ for generator $\mathbf{g} \in \mathbb{R}^2$. We define a two-dimensional function that conveys the information about the sources locations, i.e.

$$s[q,p] := \sum_{k=0}^{K-1} \frac{R_0}{R_k} \mathbf{1}_{V(q\frac{v_c}{f_s}, p\frac{2\pi}{MP})}(\mathbf{r}_k), \tag{7}$$

where the generator is given in polar coordinates and the ranges of q and p follow from the definitions above. The indicator function $\mathbf{1}_{V(q\frac{v_c}{f_s}, p\frac{2\pi}{MP})}(\mathbf{r}_k)$, takes the value 1 whenever the kth image source location falls in the qth, pth Voronoi region, and 0 otherwise. In other words, $s[q,p]$ represents the different modeled spatial locations.

2) Loudspeaker Directivity: The loudspeaker model $\gamma_0(t,\theta)$ representing the directivity of the loudspeaker is discretized as

$$v[n,p] := \gamma_0\Big(\frac{n}{f_s} - \frac{R_0 f_s}{v_c}, \frac{2\pi p}{MP}\Big), \tag{8}$$

for $n = 0,\dots,N_v-1$ and $p = 0,\dots,MP-1$.

3) Array Geometry: Microphone signals are obtained by spatial sampling of the model's continuous aperture. The microphone positions on the circular aperture are modeled as,

$$\mu[n,p] := \begin{cases} 1 & \text{if } n = \left\lceil f_s \frac{R_a}{v_c}\left(1 - \cos\left(\frac{2\pi p}{MP}\right)\right)\right\rceil, \\ 0 & \text{otherwise} \end{cases} \tag{9}$$

for $n = 0,\dots,N_\mu - 1$, where $\lceil\cdot\rceil$ denotes the ceiling operator. Analogous to (6), we express $h[n,m]$ in terms of two-dimensional and one-dimensional discrete convolutions, i.e.

$$\begin{aligned} h[n,m] = &\sum_{m'=0}^{M-1}\sum_{n_h=0}^{N_h-1} \mu\left[n - n_h, (mP - m')_{\text{mod } MP}\right] \\ &\sum_{n_v=0}^{N_v-1} v[n_h - n_v, m']s[n_v, m'] \\ =&\mu[nP,m] *_{n,m} \big(v[n,m] *_n s[n,m]\big). \end{aligned} \tag{10}$$

C. Inverse Problem

We pose the inverse problem as a linear system of equations. In this manner, we relate the vector of image locations to the linear system estimates at each of the microphones. Let us define $\mathbf{s}^{(p)}$ as a vector of size T, with elements $\mathbf{s}_q^{(p)} := s[q,p]$, and let

$$\mathbf{s} := \left[[\mathbf{s}^{(0)}]^\top, \dots, [\mathbf{s}^{(MP-1)}]^\top\right]^\top, \tag{11}$$

where $^\top$ denotes transposition. Note $\mathbf{s}$ is of size TMP. The channel impulse responses to each microphone are arranged in a vector of size $N_h M$ as

$$\mathbf{h} := \left[[\mathbf{h}^{(0)}]^\top, \dots, [\mathbf{h}^{(m)}]^\top, \dots, [\mathbf{h}^{(M-1)}]^\top\right]^\top, \tag{12}$$

where $\mathbf{h}^{(m)}$ has size N_h, with elements $\mathbf{h}_n^{(m)} := h[n,m]$; it is the vector representation of the impulse response to microphone m. The forward model is now posed as

$$\mathbf{h} = \mathbf{\Phi}\mathbf{s} + \mathbf{n}, \tag{13}$$

where $\mathbf{\Phi}$ is a matrix of size $N_h M \times TMP$ representing the operation in Eq. (10), and $\mathbf{n}$ is a noise term.

We conclude this section by showing how matrix $\mathbf{\Phi}$ is explicitly constructed. In brief we show that it has a block Toeplitz structure which, after proper zero-padding makes it amenable to implement using the FFT. We model the microphone array and the loudspeaker directivity contributions using matrices $\mathbf{A}$ and $\mathbf{D}$, respectively. Let $\mathbf{I}_N$ denote the identity matrix of size $N \times N$ and let us define the zero-padding matrix $\mathbf{W}_{a\times b}$ as

$$\mathbf{W}_{a\times b} = \begin{bmatrix} \mathbf{I}_b \\ \mathbf{0}_{a-b\times b} \end{bmatrix}, \tag{14}$$

for some positive integers $a \geq b$. Denote by $\mathbf{F}_M$ the normalized DFT matrix of size $M \times M$. Then,

$$\mathbf{\Phi} := \left(\mathbf{I}_{MN_h} \otimes \left[1, \mathbf{0}_{P-1}\right]\right) \mathbf{A}\mathbf{D} \left(\mathbf{I}_{MP} \otimes \mathbf{W}_{N_h\times T}\right). \tag{15}$$

where $\otimes$ is the Kronecker product. We give next explicit expressions for the matrices $\mathbf{A}$ and $\mathbf{D}$.

1) Loudspeaker Directivity $\mathbf{D}$*:* We form a vector by concatenating the angle-dependent directivity responses in (8)

$$\mathbf{v} := \left[[\mathbf{v}^{(0)}]^\top, \dots, [\mathbf{v}^{(p)}]^\top, \dots [\mathbf{v}^{(MP-1)}]^\top\right]^\top, \tag{16}$$

of size $N_v MP$, where $\mathbf{v}^{(p)}$ has size N_v and elements $\mathbf{v}_n^{(p)} := v[n,p]$. Then we define

$$\mathbf{D} := \left(\mathbf{I}_{MP} \otimes \mathbf{F}_{N_h}\right)^{-1} \mathbf{\Lambda}_{\mathbf{v}} \left(\mathbf{I}_{MP} \otimes \mathbf{F}_{N_h}\right), \tag{17}$$

where

$$\mathbf{\Lambda_v} := \text{diag}\left\{\left(\mathbf{I}_{MP} \otimes \mathbf{F}_{N_h}\mathbf{W}_{(N_h \times N_v)}\right)\mathbf{v}\right\}, \quad (18)$$

where $\text{diag}\{\mathbf{b}\}$ is a diagonal matrix with entries given by the elements in vector $\mathbf{b}$.

2) Array Geometry $\mathbf{A}$*:* We make a vector of size $N_\mu MP$

$$\mathbf{m} := \left[[\mathbf{m}^{(0)}]^\top, \ldots, [\mathbf{m}^{(MP-1)}]^\top\right]^\top, \quad (19)$$

where $\mathbf{m}^{(p)}$ has size N_μ, and has elements $\mathbf{m}_n^{(p)} := \mu[n,p]$. Then,

$$\mathbf{A} := \left(\mathbf{F}_{MP} \otimes \mathbf{F}_{N_h}\right)^{-1} \mathbf{\Lambda_m} \left(\mathbf{F}_{MP} \otimes \mathbf{F}_{N_h}\right), \quad (20)$$

where

$$\mathbf{\Lambda_m} := \text{diag}\left\{\left(\mathbf{F}_{MP} \otimes \mathbf{F}_{N_h}\right)\left(\mathbf{I}_{MP} \otimes \mathbf{W}_{(N_h \times N_\mu)}\right)\mathbf{m}\right\}. \quad (21)$$

D. Solution to the Inverse Problem

The solution of the inverse problem consists of extracting the image source locations $\mathbf{s}$ from the channel estimates $\mathbf{h}$, i.e. an estimation of the inverse of the forward model in Eq. (13). The system of equations in Eq. (13) is in general overdetermined since $N_h M > TMP$. It is possible to interpret $\mathbf{\Phi}$ as a large dictionary of reflections where each column captures the channel response due to a single image source. In principle, the indexes in $\mathbf{s}$ corresponding to non-zero values in the solution carry image source location information. We estimate the inverse of the forward model in Eq. (13) using two different approaches.

First note that the magnitude of delay-and-sum steered-response can be computed using $\mathbf{A}^\top$. Also the matched filter for the loudspeaker directivity response involves multiplication with $\mathbf{D}^\top$. Then, the cross-correlation delay-and-sum estimate is given by

$$\hat{\mathbf{s}}_{\text{CC-DAS}} = |\mathbf{\Phi}^\top \mathbf{h}|, \quad (22)$$

where $|\cdot|$ denotes element-wise absolute value. It is important to emphasize that this is a generalization of the methods presented in [3] and [9]. Therein, the loudspeaker is assumed omnidirectional. These approaches are known to be biased for loudspeaker impulse response mismatches and for closely spaced sources [10].

Moreover, note that the vector $\mathbf{s}$ is sparse since only a few candidate positions will be occupied by the unknown image sources. We therefore pursue a sparcity promoting solution, i.e. we write the problem as an ℓ_1-regularized least squares problem,

$$\hat{\mathbf{s}}_{\text{sparse}} = \underset{\mathbf{s} \in \mathbb{R}^{TMP}}{\arg\min} \|\mathbf{h} - \mathbf{\Phi}\mathbf{s}\|_2^2 + \lambda \|\mathbf{s}\|_1, \quad (23)$$

where $\lambda > 0$ is a regularization parameter.

III. Experimental Results

A. Setup

We evaluate the performance of the proposed algorithm in two different scenarios and compare it with other methods. We focus on two factors that influence performance. First, the assumption of an omnidirectional directivity pattern whereas the loudspeaker is directive. Second, the ability to resolve echoes whenever there exist more than one reflecting boundary. In particular, we consider the loudspeaker deconvolution techniques GCC-PHAT [12], cross-correlation delay-and-sum (CC-DAS) [3], [9], and ℓ_1-regularized least squares (LS) [7]. In GCC-PHAT localization is performed through trilateration based on the TOA estimates of the array. An overview of these methods is provided in Table I. In high quality systems, a loudspeaker with high bandwidth that radiates homogeneously in a wide angle range is desired. The directivity function used in the experiments is depicted in Fig. 2. It is obtained from measurements in anechoic conditions. In order to assess performance in estimating locations, i.e. $\hat{\mathbf{r}}$, under additive white Gaussian noise (AWGN), we have used two different metrics: the mean squared error $\text{MSE}(\hat{\mathbf{r}}) = \|\mathbf{r} - \hat{\mathbf{r}}\|^2$, and the error rate, i.e. localization is incorrect if $\|\mathbf{r} - \hat{\mathbf{r}}\|^2 > \epsilon$ for $\epsilon = 0.01$, where $\mathbf{r}$ is the true source location. The MSE and the error rate can reveal the differences in performance regarding precision and accuracy respectively, i.e. a consistent bias in the estimate against correct estimates. In the experiments, we have chosen $f_s = 48$ kHz, $R_a = 0.035$ m, and $M = 6$ microphones. The angle-dependent system impulse response $\gamma_0(t, \varphi)$ is measured for 12 uniform angles and truncated to $N_v = 50$ samples. The parameters of the image source candidate locations are set to $T = 78$ and $P = 2$ resulting in $\mathbf{h}$ having 936 entries. The value for λ parameter in Eq. (23) was determined empirically.

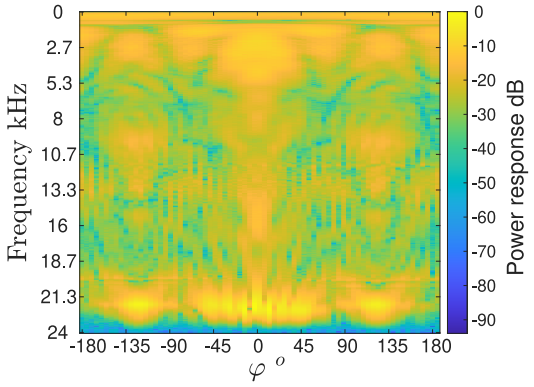

Fig. 2: Measured loudspeaker directivity function.

B. Results

1) Single Wall: In the simulations, the wall is rotated 30° around the system at a fixed distance of 0.5 m to obtain 12 wall-relative positions. This results in different DOAs and loudspeaker impulse responses. Experiments are made for each of the 12 different DOA's and 50 different noise realizations per DOA. The results here reported are averaged over the whole set of 12×50 experiments. It is also assumed that the unknown image source is exactly located at one of the predefined points of candidate locations. We expect methods assuming an omnidirectional impulse response to introduce biases when the loudspeaker is directional [3]. Indeed, Figures 3a and 3b show the results of locating a single wall versus the SNR. Methods not accounting for directionality have a fixed

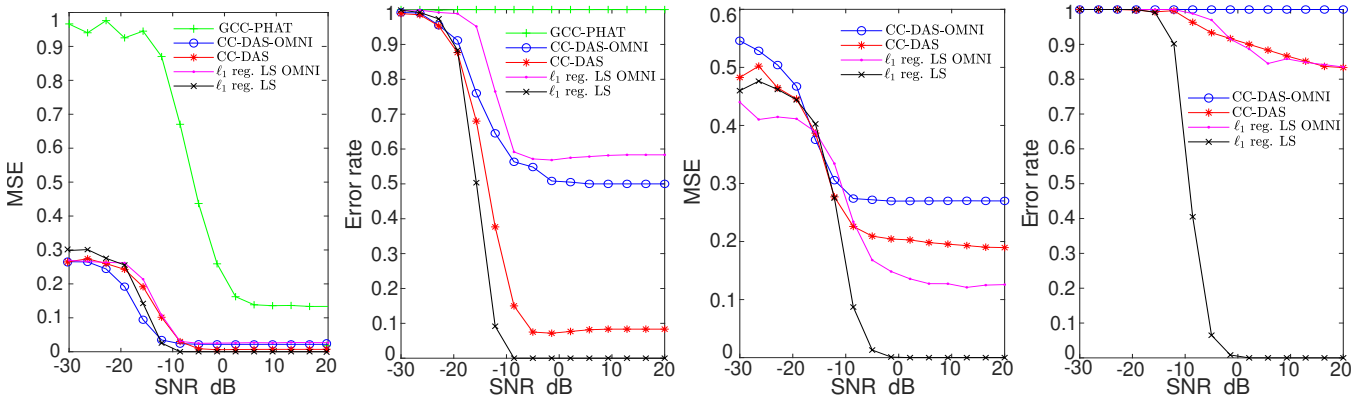

(a) Single-wall MSE (b) Single-wall error rate (c) Corner MSE (d) Corner error rate

Fig. 3: Performance comparison of various methods for localizing image sources in the presence of AWGN.

TABLE I: Comparison of methods used in experimental setup. Methods with * denote proposed.

Method	LS Model	Deconvolution	Geometric loc.
GCC-PHAT	$\gamma_0(t)$	GCC-PHAT	LS Trilateration
CC-DAS-OMNI	$\gamma_0(t)$	Cross Corr.	Delay and Sum
CC-DAS*	$\gamma_0(t,\varphi)$	Cross Corr.	Delay and Sum
ℓ_1 reg. LS OMNI	$\gamma_0(t)$	Sparse deconv.	Plane wave resp.
ℓ_1 reg. LS*	$\gamma_0(t,\varphi)$	Sparse deconv.	Plane wave resp.

bias. This manifests itself in a higher error rate. GCC-PHAT specifically has here poor performance. This can be attributed to a TOA estimation that is not geometrically constrained by the microphone locations which makes the trilateration process more sensitive. This problem is significantly reduced in the proposed directivity-aware methods, namely CC-DAS and ℓ_1-regularized LS.

2) Two Walls: We place the system in a 90°-degree corner equidistant to the two walls forming it. As before, the system is also rotated to average over several realizations. We require each of the methods to provide two location estimates. GCC-PHAT is not considered here due to its poor performance in the single-wall case and the fact that TOAs would need to be sorted out to their corresponding sources, which falls outside the scope of this work. In the two-walls case both reflections arrive very close in time at the microphones. Steered-response power methods usually have difficulty in this scenario [3], [9]. We expect sparse recovery methods to be less affected by time smearing. As can be seen in Fig. 3c and 3d, methods not considering directivity are biased. When considering only MSE it seems that to be able to correctly resolve individual echoes is more relevant than the inclusion of a directivity model, which would explain why CC-DAS methods underperform here. The bias introduced, however, hinders performance with respect to accuracy. It can be observed that ℓ_1-regularized LS consistently attains the best performance. This suggests that, by introducing a directivity model, sparse recovery methods are able to further reduce the uncertainty in echo detection.

IV. Conclusions

We present a method for robust estimation of reflecting boundaries that incorporates a loudspeaker directivity model. The times of arrival of echoes are estimated in a joint step where both microphone array geometry and loudspeaker directivity are considered. The method is shown to decrease localization error and improve the accuracy compared to cross-correlation-based methods when more than one reflecting boundaries are present. Future work can involve an extension of this method to multi-driver systems, and extending the model to account for room boundaries in three dimensions.

References

[1] F. Jacobsen and P. M. Juhl, *Fundamentals of general linear acoustics*. John Wiley & Sons, 2013.

[2] T. Betlehem and T. D. Abhayapala, "Theory and design of sound field reproduction in reverberant rooms," *The Journal of the Acoustical Society of America*, vol. 117, no. 4, pp. 2100–2111, 2005.

[3] S. Tervo, J. Pätynen, and T. Lokki, "Acoustic reflection localization from room impulse responses," *ACTA Acustica united with Acustica*, vol. 98, no. 3, pp. 418–440, 2012.

[4] M. Coutino, M. B. Møller, J. K. Nielsen, and R. Heusdens, "Greedy alternative for room geometry estimation from acoustic echoes: A subspace-based method," in *IEEE International Conference on Acoustics, Speech and Signal Processing (ICASSP)*. IEEE, 2017, pp. 366–370.

[5] I. Jager, R. Heusdens, and N. D. Gaubitch, "Room geometry estimation from acoustic echoes using graph-based echo labeling," in *IEEE International Conference on Acoustics, Speech and Signal Processing (ICASSP)*, March 2016, pp. 1–5.

[6] F. Antonacci, J. Filos, M. R. Thomas, E. A. Habets, A. Sarti, P. A. Naylor, and S. Tubaro, "Inference of room geometry from acoustic impulse responses," *IEEE Transactions on Audio, Speech, and Language Processing*, vol. 20, no. 10, pp. 2683–2695, 2012.

[7] F. Ribeiro, D. Florencio, D. Ba, and C. Zhang, "Geometrically constrained room modeling with compact microphone arrays," *IEEE Transactions on Audio, Speech, and Language Processing*, vol. 20, no. 5, pp. 1449–1460, 2011.

[8] J. B. Allen and D. A. Berkley, "Image method for efficiently simulating small-room acoustics," *The Journal of the Acoustical Society of America*, vol. 65, no. 4, pp. 943–950, 1979.

[9] A. M. Torres, J. J. Lopez, B. Pueo, and M. Cobos, "Room acoustics analysis using circular arrays: An experimental study based on sound field plane-wave decomposition," *The Journal of the Acoustical Society of America*, vol. 133, no. 4, pp. 2146–2156, 2013.

[10] T. F. Brooks and W. M. Humphreys, "A deconvolution approach for the mapping of acoustic sources (DAMAS) determined from phased microphone arrays," *Journal of Sound and Vibration*, vol. 294, no. 4-5, pp. 856–879, 2006.

[11] G.-B. Stan, J.-J. Embrechts, and D. Archambeau, "Comparison of different impulse response measurement techniques," *Journal of the Audio Engineering Society*, vol. 50, no. 4, pp. 249–262, 2002.

[12] C. Knapp and G. Carter, "The generalized correlation method for estimation of time delay," *IEEE transactions on acoustics, speech, and signal processing*, vol. 24, no. 4, pp. 320–327, 1976.